NASA TECHNICAL TRANSLATION

NASA TT F-317

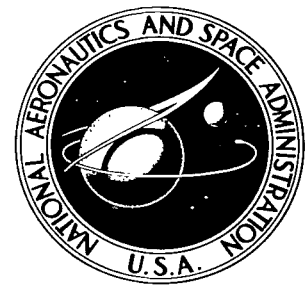

NASA TT F-317

MEASUREMENT OF THE MICROSTRUCTURE BY THE METHOD OF SMALL ANGLES

by K. S. Shifrin and V. I. Golikov

From *Trudy Glavnoy Geofizicheskoy Observatorii imeni A. I. Voyeykova,* No. 152, 1964

NATIONAL AERONAUTICS AND SPACE ADMINISTRATION • WASHINGTON, D. C. • APRIL 1965

NASA TT F-317

MEASUREMENT OF THE MICROSTRUCTURE BY THE METHOD OF SMALL ANGLES

K. S. Shifrin and V. I. Golikov

Translation of "Izmereniya mikrostruktury metodom malykh uglov." Trudy Glavnoy Geofizicheskoy Observatorii imeni A. I. Voyeykova, No. 152, pp. 3-15, 1964.

NATIONAL AERONAUTICS AND SPACE ADMINISTRATION

For sale by the Office of Technical Services, Department of Commerce, Washington, D.C. 20230 -- Price $1.00

MEASUREMENT OF THE MICROSTRUCTURE BY THE METHOD OF SMALL ANGLES

K. S. Shifrin and V. I. Golikov

ABSTRACT

The article discusses the results of testing a prototype of a field device for measuring the microstructure of fogs by the method of small angles.

Introduction

The prototype of the device for measuring the spectrum of the dimensions of fog droplets (ref. 1) was tested: (1) under laboratory conditions with calibrated models of the sol consisting of spherical particles of methyl methacrylate, (2) in artificial fogs in the chamber of the Vysokogornyy Geophysical Institute (Nal'chik-Terskol) and (3) in natural fogs (Voyeykovo). The article considers the results of these investigations and also considers the question of the accuracy and limitations of the method of small angles.

Laboratory Testing of the Device

Measurements were taken with a previously calibrated sol. Powders of AKR-100 methyl methacrylate were used consisting of transparent particles in the form of flat models--a mono-layer of particles on the surface of a glass plate--in the form of volumetric models--particles of powder suspended in a cuvette with distilled water, and subjected to continuous mixing (model of the fog).

The microstructure of AKR-100 powders was investigated by the method of direct counting under the microscope and by the method of microphotography. The data from various samples were added to obtain the averaged spectra $\overline{f(a)}$ for each fraction of the AKR-100.

In selecting the weighed portions for two-dimensional and volumetric models, it is possible to separate the particles according to their dimensions (the spectrum of an individual model may vary from the averaged spectrum of a given fraction of AKR-100). For this reason in the two-dimensional models it was necessary to carry out microphotographic investigations of the spectrum of each model while in the volumetric models it was necessary to refine the spectrum further by measuring the transmission of light in the direction $\beta = 0$ when the disturbed particles of the powder settled down. The settling took place in a cuvette with a height of $h = 550$ mm during a period of $t = 30\text{-}35$ min. In this case the variation in the transparency of the suspension was registered by photometry. From the comparisons of the curve for the variation of transparency with the data obtained from the calculation of the precipitation velocity of spherical particles from the suspension according to Stokes's Law, the distribution of spherical particles according to size was computed (refs. 2-4).

Two-dimensional models. The methodology of working with two-dimensional models of a calibrated sol is described in detail in reference 5.

To eliminate spatial non-homogeneity of the sample, it was necessary either to rotate the sample or to measure the angular distribution of the scattered light $I(\beta)$ along several diameters in the focal plane of the receiving lens and take the average value $\overline{I(\beta)}$.

Figure 1a and b shows typical spectra $f(a)$ of two-dimensional models for two fractions of the methyl methacrylate powders compared with the spectra computed by the microphotographic method.

Investigations with two-dimensional models have shown that the high stability of these models in time makes them useful for a running check of the device and of the photometer. In the case when we have several fractions of the AKR-100 powder (fine, average and coarse) with a well-studied averaged spectrum $\overline{f(a)}$, the two-dimensional models become easily reproducible. By means of such fractions it is convenient to check the proper operation of the device with small, average and large particles.

Volumetric models. The weighed portion of the powder with known spectrum of particles $\overline{f(a)}$ is lowered into distilled water contained in a cuvette with two plane-parallel glass plates for the entry and exit of light rays. The entire suspension is continuously mixed with a stirring rod driven by a vibrator (dynamic loud speaker, driven by an audio frequency generator with a vane attached to the cone or by means of an electric motor with an impeller), to prevent the precipitation of particles. In this way we obtain a stable volumetric model of fog with a known spectrum.

When we measured the spectrum $f(a)$ with a defraction device in the case of particles suspended in the medium with a refraction index which differs from the refraction index of the surrounding air, we took into account the variation of the scattering angle β when the rays entered the air from the test chamber

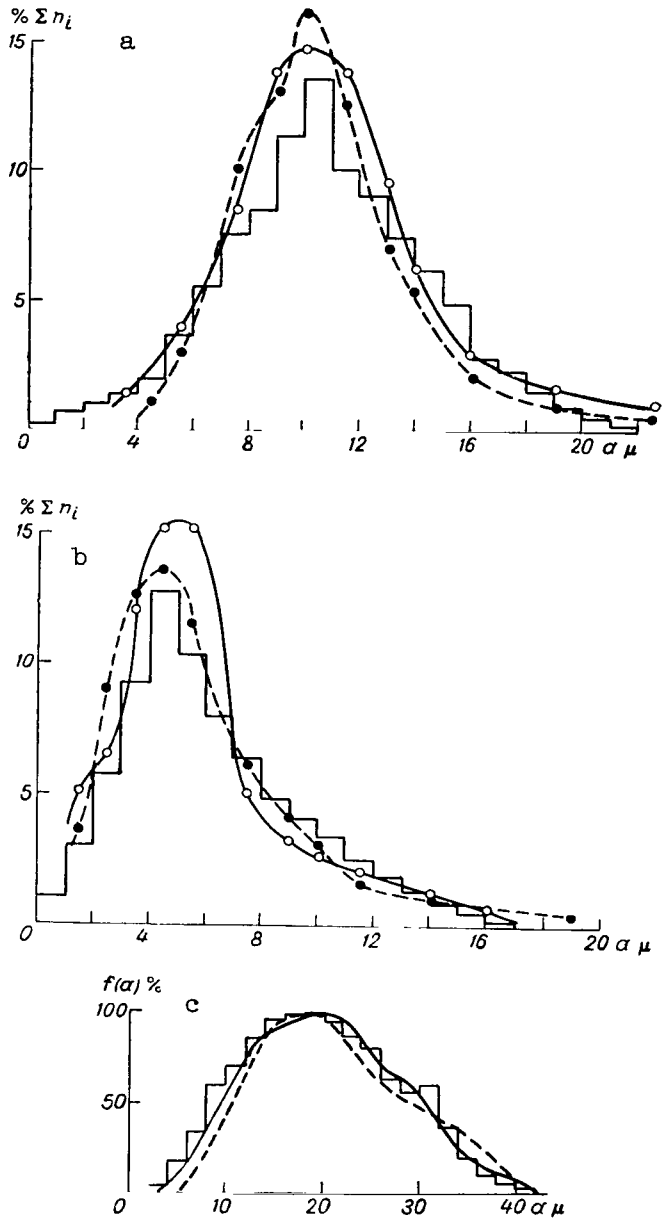

Figure 1. Spectra of dimensions of spherical methyl methacrylate particles. a, b - Two-dimensional models, c - Volumetric models. Stepwise curves are obtained by the microphotographic method, while solid and broken curves are obtained by the defraction device for measuring the structure.

$$\beta = \frac{r}{fn_w}, \qquad (1)$$

where r is the displacement of the diaphragm of the light receiver (ref. 1), n_w is the index of refraction of the water, f is the focal distance of the light-receiving lens (ref. 1).

Figure 1c shows the spectra of volumetric models of AKR-100 obtained by the method of small angles and by microphotography. In figure 1c, the left branch of f(a) shows a substantial loss of small particles due to the phenomenon of flotation: When the test chamber is insufficiently filled there is a capture of small particles by air bubbles due to the action of the agitator and the retention of these particles by the foam which forms on the surface of the water.

It was possible to eliminate the effect which produces the capture of small particles by changing the construction of the mixer (a vibrator in place of a rotating agitator) and by covering the chamber in such a way that there are no air bubbles between the cover and the surface of the water.

Measurements with models. The principal objective of the work with the calibrated sol was the evaluation of the accuracy achieved in measuring the spectrum f(a) by the device.

A series of samples of the sol with a known spectrum as determined by microphotography was investigated many times by means of the method of small angles. The results for one of such samples are shown in figure 2. Here the stepwise curve gives the spectrum of the sample obtained by the method of microphotography, the two solid lines show the possible spread of points f(a) for five consecutive measurements of $I(\beta)$.

Comparisons of this type were carried out with three forms of distribution f(a) having maxima for a equal to 6, 15, 25 microns. As was to be expected, the best reproduction was achieved for the ordinate of the spectrum f(a), lying close to the $f_{max}(a)$ to $\pm$5-10 percent from $f_{max}(a)$. Near the bases of the spectra below 0.25 f_{max} (a), the reproducibility drops to $\pm$25-35 percent.

The accuracy of reproduction of f(a) is determined by the accuracy of photometric measurements and the accuracy with which $I(\beta)$ is processed.

The accuracy of the photometric measurements was determined by a special check of the photometer with a calibrated light source using the photometric bench. It is found to be equal to 4-8 percent for the photometer's scales of 10^{-3} to 10^{-8} lumens.

The presence of calibrated fractions of the AKR-100 powders allows checking the operation of the photometer at any time.

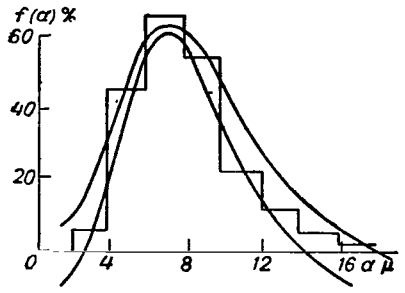

Figure 2. Reproducibility of the f(a) spectrum for the same two-dimensional model with successive measurements of illumination under small angles of scattering.

To compare the spectra of f(a) it is necessary to have a number of drops in the test samples and in the illuminated volume, sufficient to achieve a statistical filling of the spectrum f(a). In the test samples 1500-3000 particles were usually counted, while the illuminated volume was selected so that it would also have 1500-3000 droplets (ref. 1).

In comparing the relative spectra of f(a), obtained by different methods we normalized with respect to $f_{max}(a)$ and also with respect to the total number of particles. Basically the first method was used to compare the spectra of two-dimensional models in 1957-1958 (ref. 5).

The second method consisted of the following. The total number of particles was counted from a_{min} to a_{max} which was assumed to be 100 percent. From this the curve for the percentage reproducibility of f(a) was computed.

When continuous operation traps are used, the total number N of particles is usually known. However, the spectra of f(a) obtained from the defraction structure measuring device were obtained in relative units.

Therefore the comparison of such spectra was carried out over the area under the curves S proportional to N. The spectra $f_{device}(a)$ obtained by the device and $f_{trap}(a)$ obtained by the traps were constructed to a scale for which the areas under the compared curves of f(a) were the same for both methods. This means that the number of particles investigated by the trap is equal to the number of particles investigated by the device. In the case when $N \geq 1500$-3000, such an assumption is valid because, in fact, $N_{device} \gg N_{trap}$ (ref. 1).

All the relative spectra f(a) obtained by the defraction structure measuring device are constructed to the same scale and are comparable to each other (when $I(\beta)$ is processed, the transmitted light is normalized; ref. 1).

These remarks should be borne in mind when discussing the results of testing the device in artificial and natural fogs.

Testing of the Device in the Fog Chamber of the Vysokogornyy Geophysical Institute (VGI)

In October 1960 measurements of the spectra of droplets were carried out for steam fogs in the chamber of the El'bruss Expedition of VGI. The distribution of droplets according to the device was compared with the data furnished by simultaneous measurements carried out by means of continuously operating traps.

The fog in the chamber was formed by releasing approximately 500 m^3 of steam into the chamber at a pressure of 2-3 atm. The total life of the fog was 30-40 min.

The device and trap were placed close to each other at the center of the chamber. The intake of the test samples by the traps was carried out during the recording of the distribution of scattered light $I(\beta)$ approximately in the middle of the time interval necessary to record $I(\beta)$ over the angles 0-12° (ref. 1). In a series of cases test samples were taken by the traps during the entire recording cycle for $I(\beta)$ as well as during repetitive recordings of $I(\beta)$ for a period of 30-35 min, i.e., until dispersion of the fog took place. These variations in the operating conditions of the traps were carried out first to select optimum conditions for comparing the spectra given by the device and the traps, which had different information collection times, and secondly to exclude the effect of the oscillations of the microstructure of the fog (nonhomogeneity in time and in volume was noticeable), in the third place to study the variation in the microstructure of the fog from the time of its formation until its dispersion.

The results of the measurements are shown in figure 3, which shows the spectra of the traps and of the differential structure meter for different cycles of the fog. The ordinate axis shows the recurrence of the radii of droplets in percent. The sequence of the measurements of the spectra f(a) by the device and by the traps is shown by the numbers.

To count the droplets photographed on film, a special counting arrangement was used (an enlarger with a contact comb and a screen), developed at VGI.

The quantity of droplets was used to compare only the f(a) spectra measured simultaneously by the trap and by the device. Since the true value of $\Sigma n_i = N$ measured with the device during the period of measurement is unknown (the relative distributions $I(\beta)$ were recorded), the spectra f(a) according to the device were constructed on comparison graphs on the assumption that the total number of particles N_{trap} counted from the microphotographs during the operation cycle of the trap is equal to the total number of particles N_{device}

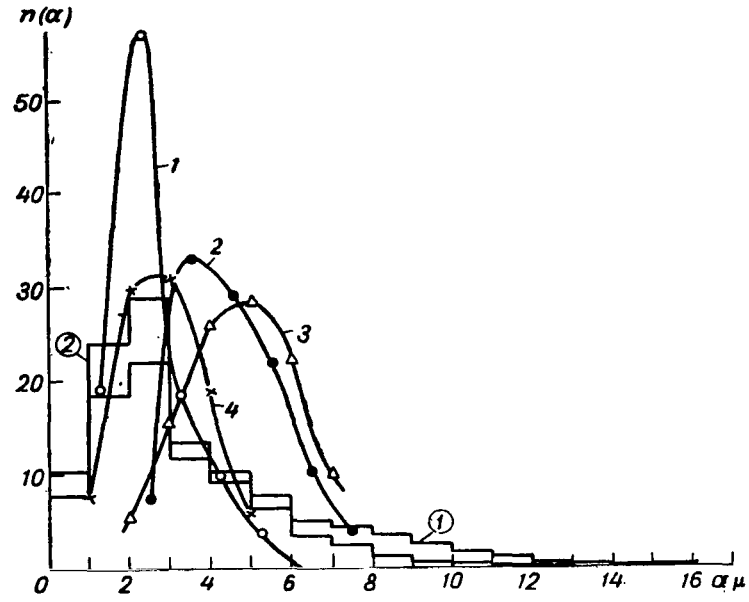

Figure 3. Comparison of the spectra of droplet dimensions by defraction structure-meter and continuous operation traps.

investigated by the device during the time of measurement of $I(\beta)$ in the entire interval of scattering angles $\beta = 0\text{-}12^{\circ}$.

The total time for the measurement of spectrum f(a) by a continuously operating trap with exposures of 0.1 sec was approximately 1 min, the total recording time of $I(\beta)$ in the interval of angles $0\text{-}12^{\circ}$ was approximately 2.5 min. The traps were turned on approximately 30-50 sec after the beginning of the recording of $I(\beta)$. In individual cases the operational cycle of the traps was extended to approximately two min, i.e., almost for the entire recording interval of $I(\beta)$.

The total investigated volume V_{trap} of the fog during the exposure time of the test glasses in the traps may be computed if we know the velocity of fog flow v = 17 m/sec, the number of exposed frames n = 60, the exposure time of each test glass $\tau = 0.1$ sec, the area of the frame S_k of approximately 1 mm^2:

$$V_t = vn_{\tau}S_k = 17 \text{ m/sec} \cdot 60 \cdot 0.1 \text{ sec} \cdot 10^{-6} \text{ m}^2. \quad (2)$$

The total amount of fog consumed during the period of measurement t_{trap} = 1 min (i.e., the volume of fog passing through the tube of the trap with an area S) is equal to

$$V_t^{(d)} = \upsilon S t_t,\ V_t^{(d)} \simeq 1\ m^3. \quad (3)$$

The same volume for the defraction structure-meter is equal to

$$V_d^{(d)} = V_k t_d = 27 \cdot 10^3\ cm^3/sec \cdot 150\ sec \simeq 4\ m^3. \quad (4)$$

The total number of particles $N = \Sigma n_i$, computed in the test samples by the trap for the construction of the spectrum of $f(a)$, was approximately 1,000-1,500 at each instance of time in the illuminated volume of the defraction structure-meter there were 1,500-3,000 particles with concentrations n not lower than 50 droplets per 1 cm^3 (ref. 1).

During the entire life of the fog its local nonhomogeneity was noticeable. Therefore if we take into account the dynamic nature of the trap and of the defraction structure-meter we may consider the coincidence of spectra on figure 3 (the simultaneously measured $f_{device}(a)$ and $f_{trap}(a)$) to be good.

The effect of the local nonhomogeneity of the fog is most pronounced in the initial stage of its formation due to the condensation of vapor and a strong temperature drop in the chamber and in the devices and also at the end due to the dispersion of the fog and the precipitation of large droplets. During these periods the superposition of the measured spectra $f_{device}(a)$ and $f_{trap}(a)$ is worse. In addition to this, in the initial stage the density of the fog is very high and the spectra $f_{device}(a)$ show the presence of a large number of small droplets so that frequently the spectrum does not have a clearly defined maximum. This is apparently due to the presence of small particles (with radii less than 1-2 microns) at the moment when the vapor is released. This even results in secondary scattering. For this reason the measurements were conducted primarily 10-15 min after the vapor was injected into the chamber.

Testing the Device in Natural Fogs

During the period May-September 1961, the spectrum of the droplets was measured in natural fogs. Four fogs of advective nature were investigated: During the night from the 12th to the 13th of May, in the morning on the 15th of September, in the morning and evening of the 27th of September at Voyeykovo.

The fogs were prolonged and stable in structure. This is particularly true of the fogs on the 15th and 27th of September which were formed during a weak wind. The fog on the 27th of September prevailed for almost the entire 24 hour period.

For comparison with the spectra $f_{device}(a)$ measured by the device, the data of microphotography were utilized which were obtained by capturing test samples

on the glass with a thin layer of transformer oil. The test samples were taken during the recording time of a series of distributions $I(\beta)$ and were immediately photographed. Thus the spectra obtained by the device during a certain interval of time Δt were compared with the microphotographic spectrum $f(a)$ averaged out over the test samples taken during the same time interval Δt.

Figure 4 shows the spectra of natural fogs as a percentage of the total number of particles (the percent recurrence of the droplet radii).

The most satisfactory coincidence of spectra $f(a)$ obtained with the two methods is observed only in the case of stable and homogeneous fogs.

To give an accurate quantitative evaluation of the closeness of the distribution curves (microphotographic and optical) illustrated by figures 1-4, we consider the coincidence of the first three instances of distribution of the average droplet radius $\bar{a} = a_1$, of the average square $\sqrt{\bar{a}^2} = a_2$, and of the average cube $\sqrt[3]{\bar{a}^3} = a_3$. They indicate the degree of closeness of the average radius of the particles, of optical transparency and liquid water content, measured by both methods, and therefore have a definite physical meaning.

The collated data are shown in Table 1. In evaluating the table we should bear in mind the remarks made above concerning the states of the fog and the dynamic nature of continuous operation traps and of the defraction structure-meter.

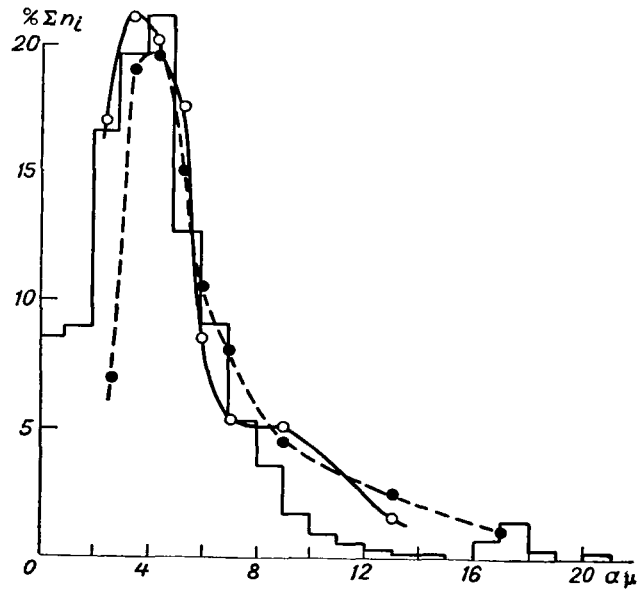

Figure 4. The spectra of natural fog (Voyeykovo).

TABLE 1

Sol sample, fog	Time, hr, min	a_1			a_2			a_3		
		"exact" values of microphoto	device	δ_1 percent	"exact" values of microphoto	device	δ_2 percent	"exact" values of microphoto	device	δ_3 percent
Two-dimensional models, 1960-1961		5.0	5.1	2.0	6.4	3.0	3.6	7.3	6.9	5.5
			5.2	4.0		1.5	0.8		7.6	4.1
		11.3	12.6	11.5	11.8	5.1	4.1	12.4	12.6	1.6
			11.2	0.9		3.3	3.8		11.8	4.8
Volumetric models, 1960-1961		20.9	20.8	0.5	22.4	22.3	0.4	23.7	23.6	0.4
			21.4	2.4		22.7	1.3		23.9	0.8
		17.9	20.4	13.9	20.5	22.3	8.8	22.6	23.9	5.7
			20.8	16.2		22.6	10.2		24.4	7.9
			20.4	3.8	22.5	21.7	3.6	23.6	22.9	2.9
		21.2	21.0	0.9		22.4	0.4		23.7	0.4
Natural fog at Voyeykovo, September 27, 1961		5.1	5.8	13.7	5.8	6.2	6.9	6.8	6.9	1.5
			6.6	29.3		7.4	27.6		8.3	22.0
Natural fog at Voyeykovo, September 27, 1961	9:45	4.4	3.9	11.4	4.9	4.2	14.3	5.4	4.3	20.4
Natural fog at Voyeykovo, May 12, 13, 1961		13.4	6.2	53.8	11.7	4.4	62.4	11.9	4.0	66.4
			5.3	60.4		3.9	66.7		3.6	69.7
			6.1	54.5		4.3	63.2		3.9	67.2
			13.9	3.7		10.1	13.7		9.3	21.8
Natural fog at Voyeykovo, September 15, 1961	9:01	8.1	7.3	9.9	8.9	8.3	6.7	9.6	8.8	8.3
	9:10		7.6	6.2		8.6	3.4		9.4	2.1
	9:17		5.5	32.1		6.9	22.5		7.8	18.8
	9:25		6.6	18.5		7.4	16.8		7.9	17.7
Artificial fog at Terskol, October 20, 1960	15:30	6.0	5.3	11.7	6.2	5.4	12.9	6.4	5.6	12.5
Artificial fog at Terskol, October 19, 1960	15:25	6.1	6.6	8.2	6.3	6.8	7.9	6.5	6.9	6.2

TABLE 1 (continued)

Sol sample, fog	Time, hr, min	a_1			a_2			a_3		
		"exact" values of microphoto	device	δ_1 percent	"exact" values of microphoto	device	δ_2 percent	"exact" values of microphoto	device	δ_3 percent
Artificial fog at Terskol, October 18, 1960	20:07	5.1	5.8	13.7	5.4	6.0	11.1	5.7	6.2	8.8
Artificial fog at Terskol, October 18, 1960	16:24	4.8	2.8	41.7	5.6	3.2	42.8	6.2	3.5	43.5
Artificial fog at Terskol, October 17, 1960	12:39	3.1	2.6	16.1	3.7	2.8	24.3	4.2	3.0	28.6
Artificial fog at Terskol, October 18, 1960	14:55	4.3	4.4	2.3	4.5	4.7	4.4	5.2	4.9	5.7
Artificial fog at Terskol, October 18, 1960	20:02	6.9	5.0	27.6	7.2	5.2	27.8	7.5	5.4	28.0
Artificial fog at Terskol, October 19, 1960	15:10	7.9	4.1	48.1	8.3	4.3	48.2	8.7	4.6	47.2
Artificial fog at Terskol, October 19, 1960	15:20	8.8	3.0	65.9	9.2	3.2	65.2	9.6	3.3	65.6
Fog chamber of MGO, 1958		4.5	4.2	6.7	5.0	4.4	12.0	5.5	4.6	16.4
Two-dimensional models, 1959-1960		19.9	13.8 15.2 17.5 11.2	30.6 23.6 12.1 43.7	13.9	11.1 10.8 13.0 8.9	20.1 22.3 6.5 36.0	12.9	11.1 10.1 12.5 8.6	14.0 21.7 31.0 33.3
Fog chamber of MGO, 1958		4.6	3.6 4.0	21.7 13.0	5.0	4.0 4.3	20.0 14.0	5.5	4.5 4.6	18.2 16.4

If we assume that all the measurements presented in Table 1 are of the same accuracy we obtain for δ the following average values in percent:

$$\bar{\delta}_1 = 20.2,\ \bar{\delta}_2 = 19.4,\ \bar{\delta}_3 = 19.9.$$

On the basis of what we have presented we may make the following conclusions.

1. As a result of the tests conducted on the field defraction structure-meter the following was verified: (a) the suitability of the device for use with natural ground fogs, (b) the stability of the device, (c) the ranges for the recording of the indicatrixes of the scattered light $I(\beta)$, (d) the accuracy of measuring the spectra of dimensions f(a) (ref. 1).

2. The spectra of dimensions f(a) of the particles with a radius of 10-30 microns and droplets of fog of 2-15 microns were measured. Approximately 350 recordings of the indicatrixes $I(\beta)$ were processed.

3. The device detects fog with a particle concentration of 50 per 1 cm^3.

4. The investigation of the "null distribution" of light I_0 near $\beta = 0$

has shown that for the spectra f(a) with a = 2-15 microns the "null distribution" may be neglected (refs. 1, 5).

5. The accuracy with which the spectrum ordinate f(a) was obtained was on the average 5-6 percent at the maximum of the curve for f(a) and approximately 25-30 percent near its base.

We should point out the extreme difficulty of processing graphically the indicatrixes $I(\beta)$. Thus during the recording of one indicatrix with PS 1-02 for a period of 2.5-10 min, its reduction in accordance with the equation of the method of small angles requires from 40 minutes to one hour (using prepared tables for $F(\beta\rho)$ and an SAR-2 computer) "Reynmetall" (or by means of an adding machine) (ref. 1).

6. During the measurements of the angular distribution of light scattered by an aerosol with an (even approximately) unknown spectrum of dimensions and concentrations, there is an uncertainty in the selection of a suitable scale of the photometer and of the velocity for the chart transport mechanism of the recorder. In the process of recording the optimum resolution, the interval of the recording angles, the sensitivity of the light sensor as a function of the spectrum f(a) and concentration vary within rather large limits. The selection of the recording ranges becomes difficult (particularly when the fog is unstable)

due to a large variation in the measured intensities of light (10^3-10^5) and due to the non-linearity of the light distribution along the angle β (ref. 1).

The result is that part of the recorded indicatrixes $I(\beta)$ is not suitable for further processing due to the impossibility of determining the exact

variation of functions $\beta^3 I$ and $\frac{d}{d\beta}(\beta^3 I)$ due to misses in the selection of the recording ranges for $I(\beta)$, which is a monotonic function of the angle β, and which does not exhibit clearly the visible pecularities in its variation associated with the microstructure (an exception to this is only the mono-dispersion systems which produce the known "crowns"). Therefore it would be desirable to observe the variation of $\beta^3 I$ and $\frac{d}{d\beta}(\beta^3 I)$ directly in the process of measuring the angular distribution of the scattered light $I(\beta)$, e.g., by means of simulation devices. A device which simulates $\beta^3 I$ and its derivative will make it possible to eliminate a stage of graphic reduction and even this will reduce the calculation time for f(a) in accordance with (4) to 20-15 min and will also eliminate the reduction of indicatrixes $I(\beta)$ which have been unfavorably recorded.

We constructed a laboratory prototype of a device which simulates $\beta^3 I$. The components of this device are being refined and it is being subjected to laboratory testing.

7. Measurements made in artificial and natural fogs have shown the necessity for a constant control of the total attenuation of light I_0, particularly in dense fogs ($n \sim 500$ droplets per cm^3 and higher). This is due to the danger of the occurrence of secondary scattering. To eliminate this the version of the device with a modulated-light signal provides for a variation in the length of the light base of the photometer (ref. 1). In natural fogs with concentrations of $n \sim 50$-100 droplets per cm^3 we may operate with a base $l_{max} \sim 10$-50 cm and even more. At the same time in dense fogs and clouds it must be reduced to 20-10 cm (concentrations $n \gg 500$ droplets per cm^3) (ref. 1).

8. Further work with the device is programmed in the following directions (ref. 1):

(a) A final transition to the scheme of a photometer with variable (modulated) light signal ("daylight" photometer);

(b) An increase in the recording speed of $I(\beta)$;

(c) An introduction of simulation and computing devices into the photometer scheme;

(d) A preparation of a prototype suitable for carrying out investigations in the environment of airplanes (the cloud microstructure);

(e) An expansion of the program for taking measurements with the defraction structure-meter in artificial and natural fogs including the comparison of the spectra of $f_{device}(a)$ with the spectra of continuous operation traps $f_{trap}(a)$;

(f) A comparison of the defraction structure-meter with all of the devices known at the present time for measuring microstructures (continuous operation traps, devices for measuring the water content, etc.).

Limitations of the Method

Let us consider questions associated with the accuracy of the method of small angles, the limit of its application, and the accuracy of measuring the spectrum of dimensions by means of the defraction structure-meter. The following limitations must be taken into account:

(a) The distribution of particles must not be very dense to eliminate the possibility of interference phenomena--the average distance between them must be greater than 5λ (λ is the wavelength of the light used). For more detail see references 1, 5, 6 and 7;

(b) The optical thickness of the illuminated object must be substantially less than unity to eliminate the possibility of secondary scattering when the theory of this method is not valid.

Let us consider the limitations in terms of particle size.

1. The lower boundary of the method. To determine the smallest radius for which we may use the method of small angles in its mathematical form as developed in refs. 8 and 9, we must have an accurate theoretical evaluation of the radii of those particles for which in the region of small angles we may definitely represent the indicatrix by the equation (refs. 8 and 9).

$$I(\beta, \lambda) = \frac{I_0}{\beta^2} \int_0^\infty J_1^2(\rho\beta) f(a) a^2 da. \tag{5}$$

Analysis of accurate calculations available at the present time shows that: 1) with an accuracy of 5-10 percent this boundary lies near $\rho = 20$; 2) when the wavelength is $\lambda = 0.5$ microns the minimum particle radius $a_m = 2$ microns. We note that there is some possibility, although it is limited by purely technical reasons, for extending the method into the region of even smaller dimensions (or at least some increase in the accuracy of the method in the region of minimum particles) by reducing the wavelength of the light (refs. 1, 5 and 7)

In Table 2 we present (according to the data of refs. 6 and 10) a comparison of the quantities

$$2i = i_1 + i_2, \tag{6}$$

computed by means of exact equations of the theory for the scattering of electromagnetic waves with the approximate values

TABLE 2

ρ	β°	2i	2i*	δ_1	Φ	Φ*	δ_2
1	2	3	4	5	6	7	8
200	0.0	$8.470 \cdot 10^8$	$8 \cdot 10^8$	5.5	0.000	0.000	0.0
	0.2	$7.461 \cdot 10^8$	$7.075 \cdot 10^8$	5.2	0.059	0.057	3.4
	0.4	$5.009 \cdot 10^8$	$4.810 \cdot 10^8$	4.0	0.196	0.192	2.0
	0.6	$2.397 \cdot 10^8$	$2.362 \cdot 10^8$	1.5	0.328	0.324	1.2
	0.8	$0.6661 \cdot 10^8$	$0.6963 \cdot 10^8$	4.5	0.401	0.398	0.8
	1.0	$0.03735 \cdot 10^8$	$0.05235 \cdot 10^8$	40.2	0.418	0.418	0.0
	1.2	$0.4922 \cdot 10^8$	$0.03318 \cdot 10^8$	93.2	0.419	0.419	0.0
	1.4	$0.1531 \cdot 10^8$	$0.1311 \cdot 10^8$	14.4	0.430	0.428	0.5
100	0.0	$5.52 \cdot 10^7$	$5 \cdot 10^7$	9.4	0.000	0.000	0.0
	0.2	$5.347 \cdot 10^7$	$4.852 \cdot 10^7$	9.3	0.016	0.015	6.3
	0.4	$4.853 \cdot 10^7$	$4.422 \cdot 10^7$	8.9	0.060	0.057	5.0
	0.6	$4.115 \cdot 10^7$	$3.777 \cdot 10^7$	8.2	0.116	0.120	3.4
	0.8	$3.240 \cdot 10^7$	$3.006 \cdot 10^7$	7.2	0.188	0.192	2.1
	1.0	$2.347 \cdot 10^7$	$2.210 \cdot 10^7$	5.8	0.299	0.301	0.7
	1.2	$1.540 \cdot 10^7$	$1.476 \cdot 10^7$	4.2	0.394	0.398	1.0
	1.4	$0.8916 \cdot 10^7$	$0.874 \cdot 10^7$	2.0	0.412	0.419	1.7
40	0	$1.282 \cdot 10^6$	$1.280 \cdot 10^6$	0.2	0.000	0.000	0.0
	1	$1.105 \cdot 10^6$	$1.132 \cdot 10^6$	2.4	0.058	0.057	1.7
	2	$0.6864 \cdot 10^6$	$0.7695 \cdot 10^6$	12.1	0.185	0.324	3.8
	3	$0.2718 \cdot 10^6$	$0.3779 \cdot 10^6$	39.0	0.293	0.398	10.6
	4	$0.04198 \cdot 10^6$	$0.1114 \cdot 10^6$	165.2	0.337	0.398	18.1
	5	$0.05292 \cdot 10^6$	$0.0084 \cdot 10^6$	84.1	0.342	0.418	22.2
	6	$0.04987 \cdot 10^6$	$0.0053 \cdot 10^6$	89.4	0.356	0.419	17.7
	7	$0.07285 \cdot 10^6$	$0.0210 \cdot 10^6$	71.2	0.397	0.428	7.8
20	0	$9.602 \cdot 10^4$	$8 \cdot 10^4$	16.7	0.000	0.000	0.0
	1	$9.205 \cdot 10^4$	$7.763 \cdot 10^4$	15.7	0.017	0.015	11.8
	3	$6.474 \cdot 10^4$	$6.043 \cdot 10^4$	6.7	0.128	0.120	6.2
	5	$2.908 \cdot 10^4$	$3.535 \cdot 10^4$	21.6	0.256	0.263	2.7

Commas represent decimal points in this table.

$$2i^* = \frac{\rho^4}{2}\left[2\,\frac{J_1(\rho\beta)}{\rho\beta}\right]^2, \tag{7}$$

obtained from the defraction equation for small scattering angles. Graph 5 shows the magnitudes of the relative error $\delta_1 = \left|\frac{i-i^*}{i}\right|$ in percent.

By examining Table 2 we may note the following two situations:

a) The large errors in δ are most often associated with the position of dark defraction rings, i.e., with the zeros of the function i^*. According to the exact theory of scattering there is no zero in this direction and it is clear that in these discrete directions the errors prove to be large;

b) Quantities i and i^* oscillate close to each other. Therefore, in the transition from the intensities to the fluxes inside the cone with a flare angle β we obtain a substantially better coincidence of the results.

Let us introduce the designation:

$$\Phi = 2\pi \int_0^{\beta} \frac{i}{\pi\rho^2} \sin\beta\, d\beta = \frac{2}{\rho^2} \int_0^{\beta} i \sin\beta\, d\beta, \tag{8}$$

$$\Phi^* = \frac{2\pi}{\pi\rho^2} \int_0^{\beta} i^* \sin\beta\, d\beta = 1 - J_0^2(\rho\beta) - J_1^2(\rho\beta) \tag{9}$$

(refs. 6 and 10).

The magnitude of $\delta_2 = \left| \frac{\Phi - \Phi^*}{\Phi^*} \right|$ in percent and also the values of Φ and Φ^* are shown in Table 2 (graphs 6-8). Here the deviation is substantially less.

In accordance with the data of Table 2 the average accuracy of the initial equation (5) for $\rho \geq 20$ may be evaluated as 5-10 percent.

2. The upper boundary of the method. The maximum radius of the particles a_{max} which may be definitely measured by the method of small angles is limited by the angular dimensions of the image of the light source in the focal plane of the light sensor and by the angular resolution of the light sensor α, necessary to record the curve showing the distribution of illumination $I(\beta)$ for a given a_{max} (ref. 1). Depending on the angular magnification of the optical part of the defraction structure-meter and the parameters of the lens of the receiving objective, a_{max} varied from 30-50 microns. Since the spectra of fogs to be measured by the defraction structure-meter in the 1960-1961 investigations are situated approximately in the interval Δa = 2-30 microns with prevalence of $f_{max}(a)$ for a = 2-15 microns (ref. 1), an optical system was used in the prototype of the device which permitted carrying out the measurements up to a_{max} = 30 microns.

Accuracy of the Method and Accuracy of the Measurements

The accuracy of the method of small angles is determined by the accuracy of the initial defraction equations, by the accuracy of the photometric measurement of the scattering indicatrixes under small angles and the accuracy of the subsequent graphical processing (refs. 5 and 7).

We have already spoken about the accuracy of the defraction equations; the error in this case is 5-10 percent.

Analysis shows that if we neglect the theoretical error (with the exception of the case when we have the smallest $\rho \simeq 30\text{-}20$) and if we assume that we do not introduce additional errors during graphic processing, then the relative accuracy for determining the ordinate of the spectrum of dimensions $\frac{\Delta f(a)}{f(a)}$ would coincide with the relative accuracy of the photometric measurements of light fluxes in the entire interval of the scattering angles. The latter depends substantially on the light flux and on the method of measuring it (refs. 1, 5 and 7).

The accuracy of photometry in the 1960-1961 measurements on the prototype of the defraction structure-meter was found to be equal to 4-8 percent (for light fluxes $\Phi_{min} = 10^{-8}$ lumens (ref. 1)).

To evaluate the accuracy of the graphical processing of experimental indicatrixes $I(\beta)$ an "arithmetic experiment" was conducted (ref. 5), which was repeated in 1960-1961. For several distributions of the form $f(a) = Aa^{\nu} e^{-\Delta a}$ for $\Delta = 0.1$, 0.2 and $\bar{a} = 15$ microns; $\Delta = 0.1$, 0.2 and $\bar{a} = 10$ microns; $\Delta = 0.1$, 0.5 and $\bar{a} = 5$ microns, the indicatrixes $I(\beta)$ were computed in accordance with equations from reference 8 and were then subjected to calculations on the basis of the equations of small angles.

Because the distribution of light intensities over the angles was known to us within the desired degree of accuracy, the deviations obtained could be attributed to the errors in graphic processing. An interval of dimensions of 2-40 microns was studied. Two calculators participated in the "arithmetic experiment." An "experienced" calculator who had previously processed graphically the experimental indicatrixes of $I(\beta)$ and an "inexperienced" operator who performed this work for the first time. It was found that for the first calculator the errors in all cases and in the entire interval of dimensions did not exceed 5 percent while for the second operator they did not exceed 10-12 percent.

Thus, the total error of the method within the limits of its applicability has three parts: the theoretical error, the photometric error, and the processing error. In the measurements described by us in references 5 and 7, it was found to be not greater than 25-30 percent during the photoelectric measurements of the fluxes of scattered light. In measurements with the defraction structure-meter the error in determining the ordinate of the spectrum of dimensions was approximately 5-6 percent near the maximum of $f(a)$ and 25-35 percent near its base. This decrease in the accuracy at the edges of distribution is due to the fact that during the graphic processing, precautions were not taken which, however, were taken in the "arithmetic experiment": the processing of the $I(\beta)$ on

large sheets of paper with a large number of intermediate points for β to a. To reduce the processing time we use the standard tables for $F(\rho\beta)$ (refs. 5, 7 and 9) and the standard intervals $\Delta\beta$ and Δa, which is what led to the processing errors of 10-12 percent.

The reproducibility of the spectrum of f(a) during a series of repetitive measurements and graphic processing is illustrated well in figure 2 (the case of the sol calibrated by the microphotographic method). We can hope that the construction of the automatic computing device and the increase in the accuracy of the photometric measurement of light fluxes will make it possible to reproduce the spectra of f(a) in the entire interval of dimensions of interest to geophysicists with an accuracy of not less than $\pm$10-15 percent.

REFERENCES

1. Golikov, V. I. Device for Measuring the Microstructure of Fogs by the Method of the Small Angles of the Scattering Indicatrix (Pribor dlya izmereniya mikrostruktury tumanov metodom malykh uglov indikatrisy rasseyaniya). (Published in the present volume).

2. Gumprecht, R. O., Sliepcevich, C. M. Measurement of Particle Sizes in Poly-Dispersed Systems by Means of Light Transmission Measurements Combined With Differential Settling. Journ. Phys. Chem., 57, No. 1, 1953.

3. Shifrin, K. S. Universal Equation for the Fall of a Sphere in a Liquid (Universal'naya formula dlya skorosti padeniya shara v zhidkosti). Izv. AN SSSR, ser. geofiz., No. 2, 1958.

4. Fuks, N. A. The Mechanics of Aerosols (Mekhanika aerozoley). Izd-vo AN SSSR, M., 1955.

5. Shifrin, K. S., Golikov, V. I. Determining the Spectrum of Droplets by the Method of Small Angles (Opredeleniye spektra kapel' metodom malykh uglov). Proceedings of the 6th inter-departmental conference on the investigation of Clouds, Precipitation and Electric Storms. Izd-vo AN SSSR, Moscow, 1961.

6. Shifrin, K. S. The Scattering of Light in a Turbid Medium (Rasseyaniye sveta v mutnoy srede). Gostekhizdat, 1951.

7. Golikov, V. I. Laboratory Set-Up for Measuring the Spectrum of the Dimensions of Spherical Particles and Fog Droplets (Laboratornaya ustanovka dlya izmereniya spektra razmerov sfericheskikh chastits i kapel' tumanov). Trudy GGO, No. 109, 1961.

8. Shifrin, K. S. The Calculation of a Class of Definite Integrals Containing the Square of the Bessel Function (Vychisleniye nekotorogo klassa opredelennykh integralov soderzhashchikh kvadrat besselevoy funktsii). Trudy VZLTI, No. 2, 1956.

9. Shifrin, K. S. The Optical Investigation of Cloud Particles (Opticheskiye issledovaniya oblachnykh chastits). Collected works "Investigation of Clouds, Precipitation and Electric Storms", Gidrometeoizdat, L., 1957.

10. Sliepcevich, C. M., Gumprecht, R. O. Scattering of Light by Large Spherical Particles. Journ. Phys. Chem., 57, No. 1, 1953.

Translated for the National Aeronautics and Space Administration
by John F. Holman and Co. Inc.

"The aeronautical and space activities of the United States shall be conducted so as to contribute . . . to the expansion of human knowledge of phenomena in the atmosphere and space. The Administration shall provide for the widest practicable and appropriate dissemination of information concerning its activities and the results thereof."

—NATIONAL AERONAUTICS AND SPACE ACT OF 1958

NASA SCIENTIFIC AND TECHNICAL PUBLICATIONS

TECHNICAL REPORTS: Scientific and technical information considered important, complete, and a lasting contribution to existing knowledge.

TECHNICAL NOTES: Information less broad in scope but nevertheless of importance as a contribution to existing knowledge.

TECHNICAL MEMORANDUMS: Information receiving limited distribution because of preliminary data, security classification, or other reasons.

CONTRACTOR REPORTS: Technical information generated in connection with a NASA contract or grant and released under NASA auspices.

TECHNICAL TRANSLATIONS: Information published in a foreign language considered to merit NASA distribution in English.

TECHNICAL REPRINTS: Information derived from NASA activities and initially published in the form of journal articles.

SPECIAL PUBLICATIONS: Information derived from or of value to NASA activities but not necessarily reporting the results of individual NASA-programmed scientific efforts. Publications include conference proceedings, monographs, data compilations, handbooks, sourcebooks, and special bibliographies.

Details on the availability of these publications may be obtained from:

SCIENTIFIC AND TECHNICAL INFORMATION DIVISION

NATIONAL AERONAUTICS AND SPACE ADMINISTRATION

Washington, D.C. 20546